中国激光

1.7 μm LD共振泵浦Tm:YAG单晶光纤激光器

董继飞[1]，王剑磊[2,4]，郑昌盛[1]，刘坚[1]，杜天一[4]，陈彬[4]，周晶晶[1]，张宁[4]，王占新[1]，赵永光[1*]，徐晓东[1]，王春[2]，徐军[3]

[1]江苏师范大学江苏省先进激光材料与器件重点实验室，江苏 徐州 221116；
[2]山东大学光学高等研究中心，山东 青岛 266237；
[3]同济大学高等研究院物理科学与工程学院，上海 200092；
[4]江苏省先进激光材料与器件国际合作联合实验室，江苏 徐州 221116

摘要 单晶光纤(SCF)具有长径比高、比表面积大、散热好等优势，近年来成为高功率激光振荡器及放大器的选择材料之一。采用光线追迹法，模拟分析了泵浦光在Tm:YAG SCF中的传播模式及强度分布情况。采用1.7 μm激光二极管(LD)作为泵浦源进行共振泵浦，将模式匹配和泵浦光导波传输结构相结合，实现了Tm:YAG SCF连续激光运转，在~2.02 μm处获得了7.85 W的功率输出，对应入射泵浦功率的斜效率为46.3%。

关键词 激光器；固体激光器；共振泵浦；Tm:YAG单晶光纤；泵浦导波

中图分类号 O436 **文献标志码** A **DOI**: 10.3788/CJL230851

1 引 言

~2 μm波段的高功率激光器可应用于激光雷达、卫星遥感等领域，且常被作为中红外光参量振荡器的泵浦源[1-4]，受到越来越多的关注。传统石英光纤由于其均匀的热分布特性，目前已成为实现高功率连续激光或高平均功率脉冲激光的主要材料[5]。然而，石英光纤中的光子变暗、非线性效应、横模不稳定性等限制了激光尤其是皮秒或飞秒脉冲激光的功率/能量的进一步提升。面对高功率/大能量激光的需求，寻找新型结构的增益介质具有重要意义。单晶光纤(SCF)是一种直径小于1 mm、典型长度为几厘米的细长晶体棒[6]。它既具有块状晶体的光谱学和热力学优势，又具有光纤的大表面积体积比。不同于传统的块状材料，单晶光纤内部的泵浦光是导波传输，而激光可以自由传输[7]。因此，单晶光纤提供了更长的增益区域，同时很好地保持了激光器的高光束质量。与传统的石英光纤相比，钇铝石榴石(YAG)SCF具有更高的热导率[YAG SCF为10.7 W/(m·K^{-1})，光纤为1.38 W/(m·K^{-1})]和更低的布里渊增益系数(YAG SCF为5×10^{-12} m/W，光纤为50×10^{-12} m/W)，因此理论上支持比石英光纤更高的临界功率[8-9]。单晶光纤已被证明是1 μm波段高平均/峰值功率激光振荡器或放大器的候选器件。2012年，法国国家科学研究中心的研究人员使用直径为1 mm、长度为40 mm的Yb:YAG SCF，获得了超过250 W的连续输出功率，功率扩展仅受可用泵浦功率的限制[10]。在超短脉冲激光放大方面，2015年，瑞士JDSU公司报道了紧凑型双程放大的Yb:YAG单晶光纤放大器，平均功率为160 W，脉宽为800 fs[11]。2014年，德国耶拿大学使用相干光束放大办法，在Yb:YAG单晶光纤中实现了光放大，当种子光的功率为6 W、重复频率6 kHz时，放大得到了输出功率为18 W、脉冲宽度为695 fs的信号光，脉冲能量为3 mJ，峰值功率达到了3.7 GW[12]。2020年，德国斯图加特大学在Yb:YAG单晶光纤中实现了超短脉冲激光放大，其中种子光功率为53 W，脉冲宽度为784 fs，重复频率为48.5 MHz，最终放大得到了输出功率为290 W、能量为6 μJ的脉冲激光输出[13]。

这些结果表明，单晶光纤在高平均功率和峰值功率方面具有巨大的应用潜力。然而，通过在单晶光纤中掺杂Tm^{3+}和Ho^{3+}稀土离子产生的2 μm激光的性能尚不明确。2020年，本课题组在微下拉法生长的Ho:YAG单晶光纤中实现了最大功率为35.2 W的2 μm连续激光输出[14]。相比之下，掺Tm^{3+}的单晶光纤可以用商用的AlGaAs激光二极管(LD)直接泵浦，受益于交叉弛豫过程，量子效率接近200%[15-16]。最近，本课题组报道了采用783 nm LD泵浦导波结构的Tm:YAG单晶光纤激光器[17]。然而，由于高量子缺陷，近红外泵浦过

收稿日期：2023-05-22；**修回日期**：2023-06-21；**录用日期**：2023-07-11；**网络首发日期**：2023-08-07
基金项目：国家自然科学基金(62075090，52032009)、江苏师范大学研究生研究与实践创新项目(2021XKT1205)
通信作者：*yongguangzhao@yeah.net

程中出现高热负载，从而限制了功率的提升。降低 Tm^{3+} 浓度虽然可减轻热负载，但会减弱交叉弛豫效应。将 Tm^{3+} 离子直接泵浦到它的激光上能级（$^3H_6\rightarrow{}^3F_4$）即共振泵浦方式，是解决这种热问题的有效方法[18-21]，并且能大大提高激光效率。

本文展示了一种简单紧凑的 1.7 μm LD 共振泵浦 Tm:YAG 单晶光纤激光器。通过光线追迹分析，研究了单晶光纤中泵浦强度分布对激光性能的影响，将模式匹配和泵浦光导波传输结构相结合，在～2.02 μm 处获得了 7.85 W 的最大输出功率，对应的斜效率为 46.3%，功率的进一步扩展仅受泵浦功率的限制。

2 实验装置

本实验采用的单晶光纤为直径为 1 mm、长度为 40 mm 的 Tm:YAG（掺杂 Tm 的原子数分数为 3.5%）SCF。为了实现更好的热效应管理，在晶体两端各键合长度为 5 mm 的未掺杂的 YAG 端帽，最终的单晶光纤总长度达到 50 mm。为了避免寄生激光振荡，两侧端帽都镀有 2 μm 波段的增透膜。

1.7 μm LD 共振泵浦 Tm:YAG SCF 激光器的实验装置图如图 1 所示，采用最大功率为 25 W、输出波长为 1.7 μm 的光纤[光纤芯径为 400 μm，数值孔径（NA）为 0.22，光束质量因子为～100]耦合半导体激光器作为泵浦源。通过光谱分析仪测量 LD 的输出波长，发现在 20 ℃的工作温度下，最大功率时的 LD 中心波长为 1719 nm。光纤耦合半导体激光器输出的泵浦光经过由透镜 L1 和透镜 L2 组成的准直聚焦系统，聚焦到单晶光纤内部。采用透镜 L1/L2 的焦距为 25.4 mm/30.0 mm 以及 30.0 mm/25.4 mm 的两种泵浦耦合方案，聚焦后泵浦光的束腰半径分别为 170 μm 和 236 μm，其焦深分别为 0.9 mm 和 2 mm。使用曲率半径为 $R=-200$ mm 的平凹镜作为输入镜（IM），采用的平面输出镜（OC）的透过率分别为 3%、5%、10% 和 15%。使用对～2.02 μm 波段高反、对 1.7 μm 波段高透的二向色镜（DM）作为泵浦光和激光束的分束器。将 Tm:YAG 单晶光纤安装在自制的水冷模块中，单晶光纤两端均采用胶水密封并在模块外突出约 1 mm，单晶光纤的整个 Tm^{3+} 掺杂部分可以直接水冷。利用 $^3H_6\rightarrow{}^3F_4$ 能级跃迁产生激光发射的掺 Tm^{3+} 激光器是准三能级系统，与室温相比，在低温下工作的激光效率更高，因此选择了 8 ℃的冷却温度。在无激光和无泵浦吸收漂白条件下，实验测得 Tm:YAG SCF 在 1.7 μm 处的单程吸收效率约为 88.6%。

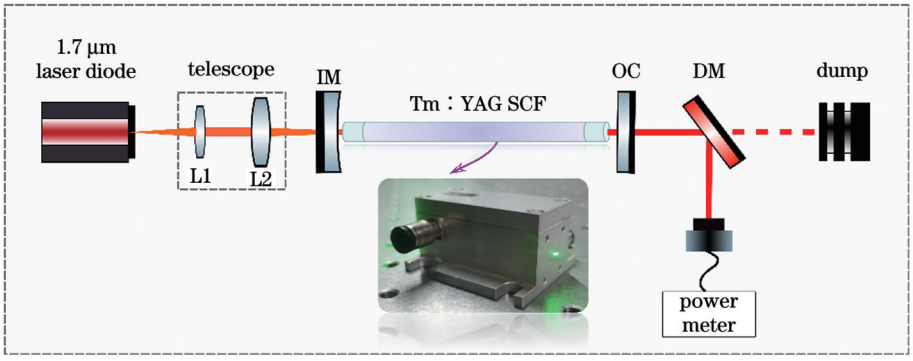

图 1 1.7 μm LD 共振泵浦 Tm:YAG SCF 激光器的实验装置，插图为自制的 Tm:YAG SCF 模块的图片

Fig. 1 Experimental setup of 1.7 μm LD resonantly pumped Tm:YAG SCF laser with picture of homemade Tm:YAG SCF module shown in inset

3 分析与讨论

首先，通过光线追迹分析模拟了泵浦光在单晶光纤中的空间强度分布，图 2(a) 显示了不同泵浦束腰半径（ω_0）下 z 轴方向（泵浦光传播方向）的强度分布。泵浦光导波传输结构使得单晶光纤的中心横截面具有更强的泵浦强度。图 2(b) 显示了两种泵浦束腰半径下单晶光纤中心区域的归一化强度分布，在单晶光纤末端，强度分别稳定在 25% 和 20% 左右。与传统的块状材料相比，在单晶光纤右侧具有相对较强的泵浦增益分布，这使得单晶光纤的泵浦增益区更长。对于两种不同的束腰半径，模拟计算得到单晶光纤中的泵浦导波区长度分别约为 44 mm 和 42 mm。通常较小的泵浦束腰半径更利于泵浦导波，且较短的焦深使得导波区长度更长。泵浦光束和腔内激光束在单晶光纤的前端都是自由传输，因此须考虑激光与泵浦光的模式匹配，选取合适的泵浦光束腰半径。

接下来在实验上分别对比了两种束腰半径下的激光输出特性。如图 2(c) 所示，对于 236 μm 的泵浦束腰半径，在单晶光纤中泵浦导波区长度为 42 mm，最大的输出功率和斜效率（η_{slope}）分别为 6.85 W 和 37.1%，分别低于泵浦束腰半径为 170 μm 时的 7.85 W 和 46.3%。后者相对更优异的激光性能归因于较好的激光模式匹配（腔内激光光束半径约为 175 μm）及较长的泵浦导波区。这表明模式匹配仍然是一个关键因素，因此要权衡泵浦导波区长度和模式匹配条件。

基于以上优化后的实验条件，当泵浦束腰半径为 170 μm 时，详细研究了物理腔长为 55 mm 的

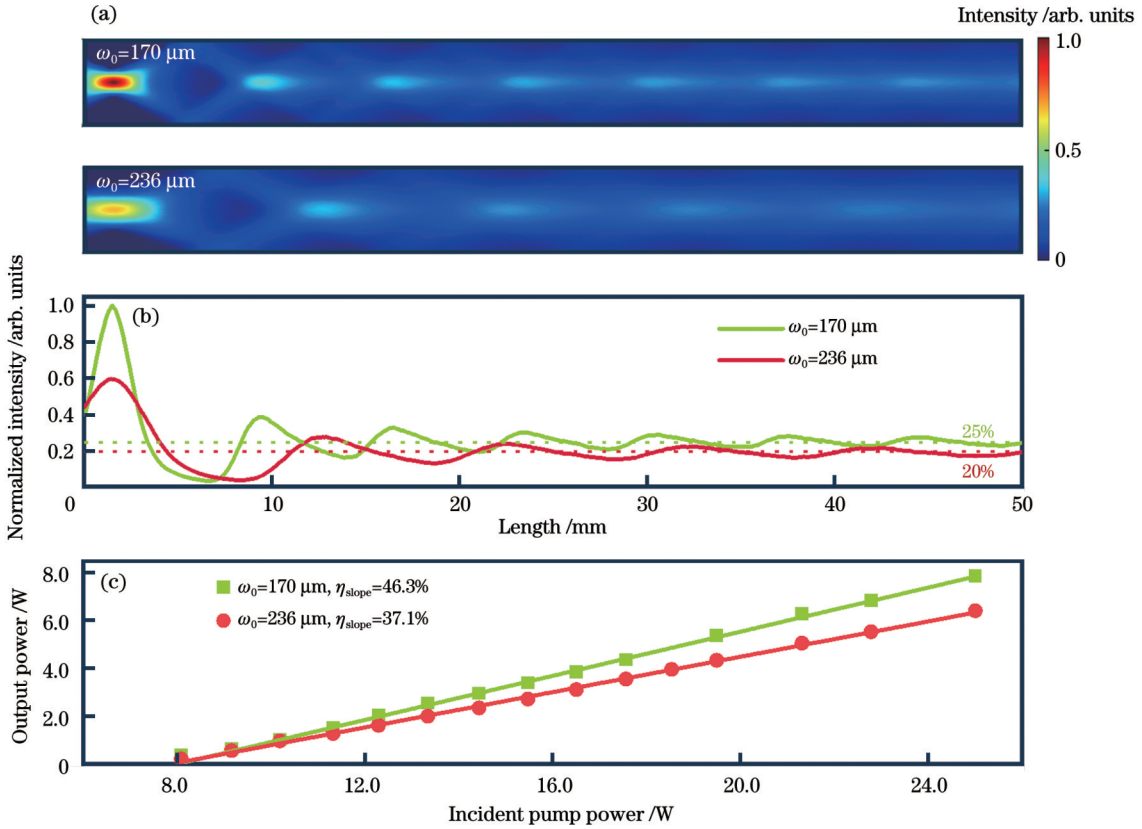

图 2 不同泵浦束腰半径下单晶光纤内的泵浦光强分布及 Tm:YAG 单晶光纤激光器的输出功率。(a)纵向截面和(b)中心轴线上的泵浦光强分布;(c)Tm:YAG 单晶光纤激光器的激光输出功率

Fig. 2 Pump intensity distributions in SCF and output powers of Tm:YAG SCF lasers under different pump beam waist radii. Pump intensity distributions on (a) longitudinal section and (b) central axis; (c) output powers of Tm:YAG SCF lasers

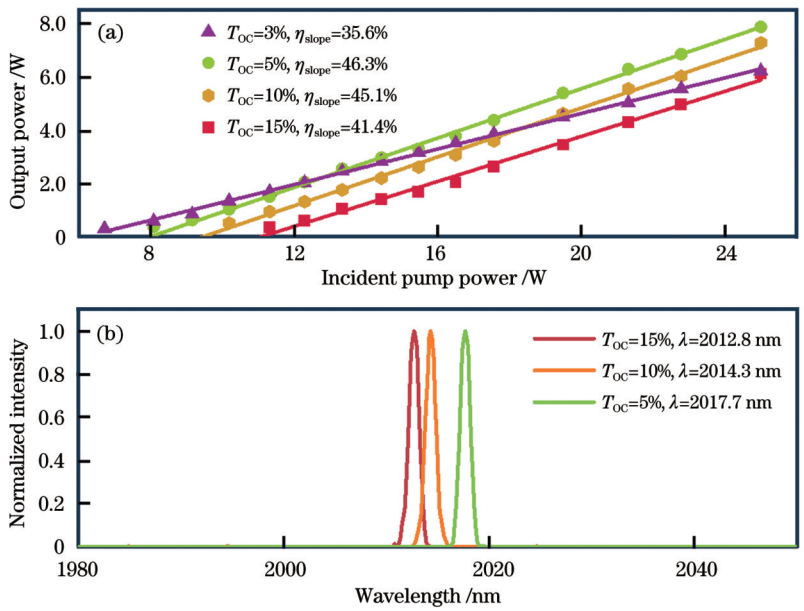

图 3 泵浦束腰半径为 170 μm 时共振泵浦 Tm:YAG SCF 激光器的连续激光输出功率以及不同输出镜下的激光光谱。(a)输出功率;(b)激光光谱

Fig. 3 Continuous laser output power of resonantly pumped Tm:YAG SCF laser with pump beam waist of 170 μm and laser spectra under different output mirrors. (a) Output powers; (b) laser spectra

Tm:YAG SCF 激光器在不同 OC 下的激光输出性能。输出功率与入射泵浦功率的关系如图 3(a)所示,当输出镜透过率(T_{OC})为 5% 时,最大输出功率为 7.85 W,对应入射泵浦功率的斜率效率为 46.3%,对应吸收泵浦功率的斜效率为 52.9%。该激光斜效率远高于 1.6 μm LD 泵浦的 Tm:LuAG 激光器(η_{slope}=33.4%)[19],

且与采用具有高光束质量的1617 nm Er:YAG固体激光器或1.6 μm Er, Yb光纤激光器作为泵浦源的Tm:YAG陶瓷激光器的效率相当(η_{slope}分别为50.1%和50%)[20-21]。另外,在实验过程中,激光输出功率与泵浦功率呈线性关系,没有观察到输出功率饱和的情况,这也说明了共振泵浦Tm:YAG SCF激光器具有输出更高功率的潜力。图3(b)为不同透过率输出镜下单晶光纤激光器的光谱。不同透过率输出镜下输出激光的波长无明显变化,T_{OC}=5%时的中心波长为2017.7 nm,随着输出镜反射率的增加,在2012.8~2017.7 nm范围内出现了约5 nm的波长红移,这是准三能级系统的典型特征,由于低透过率OC下的激光需要较低的总体反转比,故重吸收效应较强[22]。

为了评估Tm:YAG SCF激光器的光束质量,使用平凸球面透镜(焦距为100 mm)和电荷耦合器件(CCD)照相机进行了光束质量因子(M^2)的测量。图4(a)展示了不同输出功率下的横向光束质量因子(M_x^2)和纵向光束质量因子(M_y^2)。M_x^2和M_y^2的值比较接近且随着激光功率的增加而增加,这表明在SCF的横截面上热分布比较均匀。当激光输出功率为6.27 W时,测试了激光光斑半径的变化情况,如图4(b)所示,此时M_x^2=1.90,M_y^2=1.99,透镜聚焦后的焦点束腰半径分别为W=143 μm和W=146 μm。较大的光束质量因子是由于腔内没有额外的横模限制元件,高阶模没有得到抑制,故具有泵浦导波结构和长增益区的Tm:YAG SCF极易激发高阶横模[图4(c)、(d)]。因此下一步的工作重点将是优化谐振腔设计,增大基模尺寸,增加抑制高阶模的光学元件,同时保持功率的可扩展性。

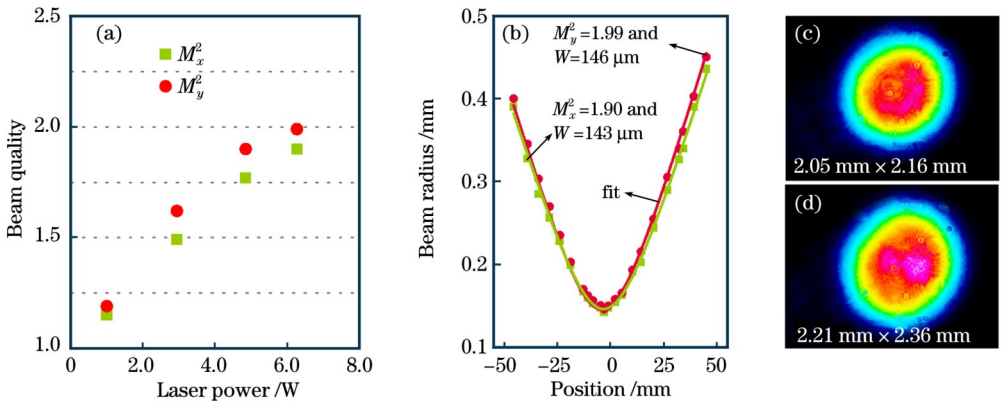

图4 共振泵浦Tm:YAG SCF激光器的光束质量。(a)不同输出激光功率下的光束质量(T_{OC}=5%);(b)典型的光束质量;(c)输出激光功率为6.27 W时的光束轮廓;(d)最大激光输出功率下的光束轮廓

Fig. 4 Beam quality of resonantly pumped Tm:YAG SCF laser. (a) Beam quality under different output powers (T_{OC}=5%); (b) typical beam quality; (c) beam profile at 6.27 W output laser power; (d) beam profile under maximum laser output power

记录距离Tm:YAG SCF激光器25.7 cm处的光斑直径大小,根据不同泵浦功率下输出激光束的M^2确定热透镜焦距的大小。由于直接水冷的均匀散热方式,单晶光纤在x、y轴方向上的热透镜焦距接近,因此仅展示了x轴方向上的随泵浦功率(P_{pump})变化的热透镜焦距,如图5所示。实验数据与理论热透镜拟合曲线吻合良好[23],理论热透镜焦距$f_{theory}=1/(\alpha P_{pump}+\beta)$,其中$\alpha$和$\beta$为常数。根据拟合曲线,估算出当最大入射泵浦功率为25 W,即输出功率为7.85 W时,热透镜焦距为62 mm。较小的热透镜焦距表明热效应依然很严重,这主要是由于单晶光纤前端部分的高泵浦吸收。较低的Tm^{3+}浓度或较长的单晶光纤可以改善纵向温度分布的均匀性,从而使激光器在更高的功率水平下运转。

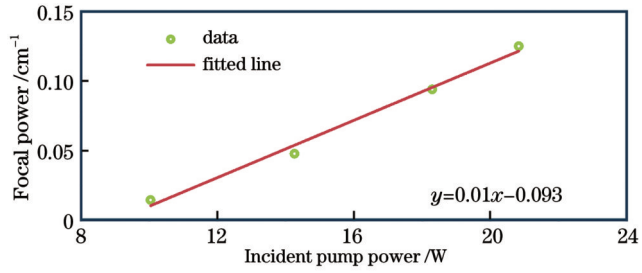

图5 热透镜焦距与入射泵浦功率的关系

Fig. 5 Focal length of thermal lens versus incident pump power

4 结 论

研究了1.7 μm LD共振泵浦Tm:YAG SCF的激光性能。通过光线追迹分析了具有不同束腰半径的泵浦光在直径为1 mm的单晶光纤中的传播情况。得益于共振泵浦方案和单晶光纤独特的优异散热性能,最终在~2.02 μm波段实现了最高功率为7.85 W的激光输出,斜效率为46.3%。在实验过程中,除了泵浦导波结构外,模式匹配也是影响单晶光纤激光性能的关键因素。理论分析结果表明,在单晶光纤的前段中,较高的泵浦强度可能会导致激光腔的不稳定。直径更细的单晶光纤或一些特殊的设计(如无掺杂端帽键合)可以进一步增强泵浦导波能力,减小单晶光纤

中的热应力，这也是目前研究的热点[24-25]。因此，未来的工作将集中在降低掺杂浓度、增加单晶光纤长度方面，进一步拓展 Tm∶YAG 单晶光纤激光器的功率范围。

参 考 文 献

[1] Dergachev A, Armstrong D, Smith A, et al. 3.4-μm ZGP RISTRA nanosecond optical parametric oscillator pumped by a 2.05-μm Ho∶YLF MOPA system[J]. Optics Express, 2007, 15(22): 14404-14413.

[2] Walsh B M. Review of Tm and Ho materials; spectroscopy and lasers[J]. Laser Physics, 2009, 19(4): 855-866.

[3] Boyd D S, Petitcolin F. Remote sensing of the terrestrial environment using middle infrared radiation (3.0-5.0 μm)[J]. International Journal of Remote Sensing, 2004, 25(17): 3343-3368.

[4] 吴鸿春. Tm∶YLF 激光腔内泵浦 2.1 μm Ho∶YVO_4激光器[J]. 中国激光, 2022, 49(23): 2301009.
Wu H C. Tm∶YLF laser intracavity pumped 2.1 μm Ho∶YVO_4 laser[J]. Chinese Journal of Lasers, 2022, 49(23): 2301009.

[5] Jauregui C, Limpert J, Tünnermann A. High-power fibre lasers [J]. Nature Photonics, 2013, 7(11): 861-867.

[6] Sangla D, Martial I, Aubry N, et al. High power laser operation with crystal fibers[J]. Applied Physics B, 2009, 97(2): 263-273.

[7] Délen X, Aubourg A, Deyra L, et al. Single crystal fiber for laser sources[J]. Proceedings of SPIE, 2015, 9342: 934202.

[8] Dawson J W, Messerly M J, Heebner J E, et al. Power scaling analysis of fiber lasers and amplifiers based on non-silica materials [J]. Proceedings of SPIE, 2010, 7686: 768611.

[9] Parthasarathy T A, Hay R S, Fair G E, et al. Predicted performance limits of yttrium aluminum garnet fiber lasers[J]. Optical Engineering, 2010, 49(9): 094302.

[10] Délen X, Piehler S, Didierjean J, et al. 250 W single-crystal fiber Yb∶YAG laser[J]. Optics Letters, 2012, 37(14): 2898-2900.

[11] Markovic V, Rohrbacher A, Hofmann P, et al. 160 W 800 fs Yb∶YAG single crystal fiber amplifier without CPA[J]. Optics Express, 2015, 23(20): 25883-25888.

[12] Kienel M, Müller M, Demmler S, et al. Coherent beam combination of Yb∶YAG single-crystal rod amplifiers[J]. Optics Letters, 2014, 39(11): 3278-3281.

[13] Beirow F, Eckerle M, Graf T, et al. Amplification of radially polarized ultra-short pulsed radiation to average output powers exceeding 250 W in a compact single-stage Yb∶YAG single-crystal fiber amplifier[J]. Applied Physics B, 2020, 126(9): 148.

[14] Zhao Y G, Wang L, Chen W D, et al. 35 W continuous-wave Ho∶YAG single-crystal fiber laser[J]. High Power Laser Science and Engineering, 2020, 8(2): e25.

[15] Honea E C, Beach R J, Sutton S B, et al. 115-W Tm∶YAG diode-pumped solid-state laser[J]. IEEE Journal of Quantum Electronics, 1997, 33(9): 1592-1600.

[16] 樊雨晴, 施翔春, 刘晶, 等. 2 μm 波段单掺铥脉冲固体激光器研究进展[J]. 激光与光电子学进展, 2023, 60(7): 0700003.
Fan Y Q, Shi X C, Liu J, et al. Research progress of Tm-doped pulsed solid-state lasers in 2 μm band[J]. Laser & Optoelectronics Progress, 2023, 60(7): 0700003.

[17] Liu J A, Dong J F, Wang Y Y, et al. Tm∶YAG single-crystal fiber laser[J]. Optics Letters, 2021, 46(18): 4454-4457.

[18] 陶蒙蒙, 叶锡生, 叶景峰, 等. 同带泵浦千瓦级掺铥光纤激光器输出特性理论模拟[J]. 中国激光, 2022, 49(1): 0101019.
Tao M M, Ye X S, Ye J F, et al. Modeling In-band pumped kW level high-power Tm-doped fiber lasers via simulations[J]. Chinese Journal of Lasers, 2022, 49(1): 0101019.

[19] Duan X M, Guo X S, Yao B Q, et al. Efficient Ho∶CaF_2 laser intracavity-pumped by a Tm∶LuAG laser in-band pumped at 1.6 μm[J]. Laser Physics Letters, 2018, 15(9): 095802.

[20] Liu J, Shen D Y, Huang H T, et al. Highly efficient Tm-doped yttrium aluminum garnet ceramic laser based on the novel fiber-bulk hybrid configuration[J]. Applied Physics Express, 2013, 6(9): 092107.

[21] Liu X L, Huang H T, Shen D Y, et al. Highly efficient resonantly pumped 2000 nm Tm∶YAG ceramic laser[J]. Optical Engineering, 2014, 53(4): 040501.

[22] Zhao Y G, Zhou W, Xu X D, et al. Spectroscopic properties and pulsed laser performance of thulium-doped $(Lu, Y)_3Al_5O_{12}$ mixed crystal[J]. Optical Materials, 2016, 62: 701-705.

[23] Kapoor R, Mukhopadhyay P K, George J, et al. Thermal lens measurement technique in end-pumped solid state lasers: application to diode-pumped microchip lasers[J]. Pramana, 1999, 52(6): 623-629.

[24] Liu B, Ohodnicki P R. Fabrication and application of single crystal fiber: review and prospective[J]. Advanced Materials Technologies, 2021, 6(9): 2100125.

[25] Qian G Q, Wang W L, Tang G W, et al. Tm∶YAG ceramic derived multimaterial fiber with high gain per unit length for 2 μm laser applications[J]. Optics Letters, 2020, 45(5): 1047-1050.

1.7 μm LD Resonantly Pumped Tm∶YAG Single Crystal Fiber Laser

Dong Jifei[1], Wang Jianlei[2,4], Zheng Changsheng[1], Liu Jian[1], Du Tianyi[4], Chen Bin[4], Zhou Jingjing[1], Zhang Ning[4], Wang Zhanxin[1], Zhao Yongguang[1*], Xu Xiaodong[1], Wang Chun[2], Xu Jun[3]

[1]*Jiangsu Key Laboratory of Advanced Laser Materials and Devices, Jiangsu Normal University, Xuzhou* 221116, *Jiangsu, China*;

[2]*Center for Optics Research and Engineering, Shandong University, Qingdao* 266237, *Shandong, China*;

[3]*School of Physics Science and Engineering, Institute for Advanced Study, Tongji University, Shanghai* 200092, *China*;

[4]*Jiangsu Advanced Laser Materials and Devices International Cooperation Joint Laboratory, Xuzhou* 221116, *Jiangsu, China*

Abstract

Objective High-power lasers within the 2-μm spectral range have been utilized in various applications in the fields of laser radar and satellite remote sensing, essentially serving as pump sources for optical parametric oscillators. Tm/Ho-doped fiber lasers are currently the primary methods for achieving high-power continuous-wave lasers or high-average-power pulsed lasers with high repetition rates

owing to their homogeneous heat load distribution. However, photon dark effects, nonlinear effects, and transverse mode instability in fibers present as obstacles for further power/energy scaling, particularly for pico- or femtosecond-pulsed lasers. To tackle these challenges in the domain of high-power lasers, the introduction of gain media with novel structures is imperative and constitutes a popular area of research. Single-crystal fibers (SCFs) are long, thin crystalline rods, typically having a diameter of less than 1 mm and length of a few centimeters. Owing to their high thermal conductivities and low Brillouin gain coefficients, SCFs combine the advantages of both bulk crystals and glass fibers. Thus, they are promising candidates for high-power laser systems.

SCFs have been showcased as promising candidates for high-average or peak-power laser oscillators and amplifiers within the 1 μm spectral region. Nevertheless, research on the laser performance of SCFs in the mid-infrared 2 μm spectral range, particularly when doped with Tm^{3+} or Ho^{3+} ions, is limited. Recently, the first Tm∶YAG SCF laser, utilizing a 783-nm pump, was reported. Owing to high quantum defects, the use of near-infrared pumping results in a significant thermal load, thereby limiting its potential for power scalability. However, by directly pumping Tm^{3+} ions into the upper laser level ($^3H_6 \rightarrow {}^3F_4$), the issue of thermal loading can be effectively addressed, thus paving the way for further power scaling and enhanced laser efficiency.

Methods The experimental setup is shown in Fig. 1. The pump source is a fiber-coupled laser diode (LD) at 1719 nm, with a maximum output power of 25 W, numerical aperture of 0.22, beam quality factor (M^2) of approximately 100, and core diameter of 400 μm. The fiber output is focused into the SCF with a variable magnification ratio depending on the telescope system, which consists of a collimating lens (L1) and focusing lens (L2). The focal lengths L1 and L2 are 25.4 mm /30.0 mm and 30.0 mm/25.4 mm for the two pump-coupling schemes. Therefore, the pump beam waist radius is either 236 μm or 170 μm within the SCF. The single crystal fiber used in this experiment is a Tm∶YAG SCF with a diameter of 1 mm and a length of 40 mm (the atomic fraction of doped Tm is 3.5%). For better thermal effect management, undoped YAG caps with bonding lengths of 5 mm at each end of the crystal are used. In order to avoid parasitic laser oscillation, both end caps are coated with 2 μm band anti-reflection films. The Tm∶YAG SCF is mounted on a custom-made aluminum module (Fig. 1), and both ends of the SCF are sealed with glue, leaving a small protrusion of approximately 1 mm outside the module. This arrangement allows the entire Tm-doped section of the SCF to be directly water-cooled to approximately 8 ℃. A planoconcave mirror with a radius of curvature of −200 mm serves as the input mirror (IM). Plane-wedged mirrors with transmittance values of 3%, 5%, 10%, and 15% are used as the output coupler (OC). A dichroic mirror (DM) functions as the beam splitter for the pump and laser beams. The propagation mode and intensity distribution of the pump light within the SCF are simulated and analyzed using the ray tracing method [Figs. 2(a) and (b)].

Results and Discussions Initially, the laser performance under different pump-guiding conditions is investigated. As shown in Fig. 2(c), with a 170-μm pump beam waist, the peak slope efficiency achieved is 46.3%. Next, the Tm∶YAG SCF laser performance with different OCs and a pump beam waist of 170 μm is examined in detail. An optimal OC with transmittance (T_{OC}) of 5% yields a maximum output power of 7.85 W, correlating to slope efficiencies of 46.3% and 52.9% with respect to the incident pump power and absorbed pump power, respectively [Fig. 3(a)]. Figure 3(b) presents the optically measured spectra for different OCs, with the laser wavelength at T_{OC}=5% situated at 2017.7 nm. A red-shift in the wavelength from 2012.8 nm to 2017.7 nm is observed with decreasing OC transmission. Figure 4(a) shows the M^2 for various output powers. Within the measured range, the M^2 value gradually increases from 1.2 to 1.9; a typical beam quality measurement in the latter case is exhibited in Fig. 4(b). The degradation in beam quality can be attributed to the excitation of higher-order transverse modes because no component for mode limitation is used in the cavity. Figure 5 represents the calculated thermal lens focal lengths along the x-axis for different incident pump powers. The focal length at the peak pump power of 25 W, corresponding to 7.85 W output laser power, is estimated to be 62 mm.

Conclusions In conclusion, a 1.7-μm LD is used as the pump source for resonant pumping, and the continuous laser operation of Tm∶YAG SCF is realized by integrating mode matching and pump guiding. This approach generates an output power of 7.85 W at approximately 2.02 μm, which corresponds to a slope efficiency of 46.3%. In addition to pump guidance, we find that mode matching also plays a crucial role in laser performance of such a 1-mm diameter SCF. Nevertheless, a theoretical analysis of the thermal lens suggests that a higher pump intensity in the front segment of the SCF may trigger instability in the laser cavity. Certain specific designs (e.g., undoped end caps) can further bolster the pump guidance and alleviate the thermal stress of the SCF.

Key words lasers; solid state lasers; resonant pumping; Tm∶YAG single-crystal fiber; pump guiding